NASA TECHNICAL
MEMORANDUM

NASA TM X-62,046

NASA TM X-62,046

COMPARISON OF PREDICTED AND MEASURED AERODYNAMICS OF A DELTA
BODY ORBITER

John B. McDevitt

Ames Research Center
Moffett Field, Calif. 94035

August 1971

COMPARISON OF PREDICTED AND MEASURED
AERODYNAMICS OF A DELTA BODY ORBITER

By

John B. McDevitt

ABSTRACT

The applicability of existing theoretical methods for estimating
the hypersonic aerodynamic characteristics of a lifting-body space shuttle
orbiter has been studied. The delta-body orbiter proposed by Lockheed
(Model LS-200-5) was used in this study. The Hypersonic Arbitrary Body
Program (HABP) of Gentry and Smyth was used for estimating the performance
of the basic vehicle, and Newtonian and "embedded flow" concepts were
used for estimating control effectiveness. The predicted characteristics
were compared with experimental measurements made in the Langley Continuous
Flow Hypersonic Tunnel at a free-stream Mach number of 10.4 and in the
Ames 3.5-foot hypersonic tunnel at a Mach number of 7.4. In general,
the HABP method provided good estimates of aerodynamic characteristics at
angles of attack less than about 30° but overpredicted somewhat the force
coefficients at large angles of attack. The "embedded flow" approach
provided the best estimates of aerodynamic control effectiveness, as
expected, although Newtonian estimates were also reasonably accurate.

INTRODUCTION

At hypersonic speeds simple theoretical methods are available which
have been found to provide good estimates of aerodynamic characteristics
for blended delta-wing designs. This was demonstrated in presentations
at the Space Transportation System Technology Symposium (Ref. 1) for the
North American Rockwell Orbiter and at the NASA Space Shuttle Technology
Conference (Ref. 2) for the McDonnell-Douglas Orbiter. The use of a
relatively compact lifting-body design for the shuttle orbiter has also been
proposed by the Lockheed Corp. and the present paper presents some
theoretical-experimental correlations for the Lockheed vehicle.

NOTATION

C_D drag coefficient, $\dfrac{\text{drag}}{q_\infty S}$

C_L lift coefficient, $\dfrac{\text{lift}}{q_\infty S}$

C_l rolling-moment coefficient, $\dfrac{\text{rolling moment}}{q_\infty S l}$

C_m pitching-moment coefficient, $\dfrac{\text{pitching moment}}{q_\infty S l}$

C_n yawing-moment coefficient, $\dfrac{\text{yawing moment}}{q_\infty S l}$

l reference length

L/D lift-drag ratio

M_∞ free-stream Mach number

q_∞ free-stream dynamic pressure

Re_{∞_l} free-stream Reynolds number based on model length

S reference area

α angle of attack (relative to model flat lower surface)

β angle of sideslip (positive nose to the left)

$\Delta(\ )$ increment quantities

$(\ )_\beta$ derivative with respect to β at $\beta = 0$.

CONFIGURATION

A sketch of the proposed Lockheed space shuttle orbiter is presented in figure 1. The vehicle is a delta lifting-body design of compact shape with high volumetric efficiency. Longitudinal control is provided by upper and lower flaps and by elevons (attached to the end of the lower flap) which can also be differentially deflected as ailerons. Twin vertical stabilizers, containing both rudders and speed brakes, provide directional stability and control. Further details regarding the design of this vehicle may be found in Ref. 3.

COMPARISONS OF PREDICTED AND MEASURED
AERODYNAMIC CHARACTERISTICS

The hypersonic experimental characteristics of the Lockheed orbiter are presented in Ref. 4. The tests were made in the NASA-Langley Continuous Flow Hypersonic Tunnel at a free-stream Mach number of 10.4, and in the NASA-Ames 3.5-foot hypersonic tunnel at a free-stream Mach number of 7.4. The Langley tests provided data at angles of attack up to about 30°, and the Ames tests extended the angle of attack range up to about 47°.

Although some estimated results for the basic vehicle (controls undeflected) were included in Ref. 4, the present paper presents a more detailed comparison of estimated and measured aerodynamic characteristics including three examples of deflected controls: (a) deflection of the lower trim flap (see figure 1), (b) differential deflection of the elevons, and (c) deflection of the rudders.

The theoretical estimates presented in this report for the basic vehicle shape (undeflected controls) were obtained (courtesy of Mr. H. H. Drosdat and Mr. F. A. Velligan of the Lockheed Missiles and Space Co.) by application of the Hypersonic Arbitrary Body Program (HABP) of Gentry and Smyth, Ref. 5. Estimates of the various control effectivenesses were made by applying "Newtonian" and "embedded flow" concepts (the HAB-Program was not used for reasons discussed later in this report).

Lift Coefficient and Lift-Drag Ratio

Comparisons of predicted and measured lift coefficient and lift-drag ratio are presented in figure 2. The theoretical estimates shown in this figure were obtained by applying the HAB-Program with "tangent-cone", "Newtonian" options used for compression surfaces and an application of the "Van Dyke Unified Method" on expansion surfaces. Estimates for the skin friction (for free-stream conditions approximating those for the Langley tests) were included since friction forces affect the lift-drag ratio noticeably at low angles of attack. The estimated lift-drag ratio agrees closely with experiment throughout the angle-of-attack range. The estimated lift coefficients also agreed closely with measurements at low angles of attack but were overpredicted at large angles of attack. This is a consequence of the flow field becoming subsonic near virtually the entire lower surface of the vehicle at large angles of attack and the loading is overpredicted in the regions of rapid flow acceleration over the swept leading edges (A similar result is the overprediction by modified Newtonian theory of the drag on the blunt entry face of the Apollo vehicle where subsonic flow accelerates rapidly to supersonic flow in the shoulder region.)

Control Effectiveness

Comparisons of calculated and measured pitching-moment coefficients are presented in figure 3 for various deflections of the lower trim flap. The Hypersonic Arbitrary Body Program was used to estimate only the zero control deflection case. For deflected controls, the HABP methods are applicable only when Newtonian (or tangent cone) concepts apply since no provisions are made to approximate the tip effects for low-aspect-ratio surfaces. Although the HABP method includes the effects of flow separation ahead of deflected controls, only two-dimensional boundary layers are considered, whereas the separation phenomenon is strongly affected by tip effects for low-aspect-ratio surfaces (see Ref. 6). In the present study this phenomenon was not considered for lack of an adequate prediction technique.

For deflections of the lower trim flap (see figure 1), incremental moments were calculated by "Newtonian" (obtained by the method described in APPENDIX A of Ref. 7) and by an "embedded flow" concept (Ref. 8) which assumed in the present case a dual body-control shock system but with reduced loading in the local regions of the Mach cones from the control tips. (The pressure coefficients in the tip regions were crudely approximated by straight-line variations from the two-dimensional-flow value to zero at the control's side edges.) The latter method is applicable, only so long as the flow remains supersonic and thus is restricted to moderate angles of attack.

In general, the estimated values shown in figure 3 agree reasonably well with the measured values. For this vehicle, simple theories provide reasonably accurate estimate of the pitch-flap effectiveness.

Comparisons of estimated and measured rolling-moment coefficient, C_l, and yawing-moment coefficient, C_n, are presented in figure 4 for the elevons deflected differentially and for the rudders deflected. The simple theories provide reasonably good approximations for the elevon effectivenesses. The measured rudder effectiveness agrees well with simple Newtonian at low angles of attack but not at high angles of attack where the flow has become subsonic in the region of the flat undersurface of the vehicle.

Lateral-Directional Stability

Comparisons of the measured and predicted yawing-moment and rolling-moment derivatives C_{n_β}, and C_{l_β} (body axes), are presented in figure 5 for the basic vehicle (controls undeflected). Also included in this figure is a theoretical-experimental correlation of the dynamic stability parameter

$$C_{n_{\beta_{dyn}}} = C_{n_\beta} \cos\alpha - \frac{I_Z}{I_X} C_{l_\beta} \sin\alpha$$

(where I_Z/I_X can be expected to be about 5 for this vehicle) which is an important flight parameter to consider for lifting bodies at angle of attack (Ref. 9). At angles of attack up to about 30° the HABP methods provide good estimates of the stability levels including the angles of attacks for changes in stability sign. However, at angles of attack greater than about 30° the theory tends to overpredict the stability level (note in particular C_{n_β} vs α).

CONCLUDING REMARKS

The present study indicates that the Hypersonic Arbitrary Body Program may be used to provide good estimates of the hypersonic aerodynamic force and moment characteristics of the lifting delta-body shape at angles of attack up to about 30°. At larger angles of attack, where the flow adjacent to the undersurface is subsonic, the theory fails to cope with the complex mixed flow problem and overpredicts the vehicle aerodynamic forces, although the ratio of lift to drag is predicted well.

Estimates of the effectiveness of various controls in the present study were made using Newtonian and "embedded flow" concepts and, although the embedded flow approach provided the best estimates, as expected, the Newtonian estimates were also reasonably good. The HABP methods should be used with caution for estimating control effectiveness since no procedures are included for estimating tip effects when low-aspect-ratio control surfaces are used.

REFERENCES

1. Katzen, E. D., Marvin, J. G., Seegmiller, H. L., Axelson, J. A., Brownson, J. J., Cleary, J. W., Lockman, W. K., and Kaattari, G. E.: Static Aerodynamics, Flow Fields and Aerodynamic Heating of Space Shuttle Orbiters. Space Transportation System Technology Symposium, NASA TM X-52876, Vol. I, 1970, pp. 142-193.

2. Hamilton, Richard K.: Correlation of Space Shuttle Applicable Experimental Hypersonic Aerodynamic Characteristics with Theory. NASA Space Shuttle Technology Conference, NASA TM X-2272, Vol. I, 1971, pp. 455-492.

3. Alexander, Grover L.: A potential Space Shuttle Orbiter. NASA Space Shuttle Technology Conference, NASA TM X-2272, Vol. I, 1971, pp. 493-537.

4. McDevitt, John B, and Mellenthin, Jack A.: Hypersonic Aerodynamic Characteristics of a Delta Body Space Shuttle Orbiter. NASA TM X-62,034, 1971.

5. Gentry, Arvel E., and Smyth, Douglas N.: Hypersonic Arbitrary-Body Aerodynamic Computer Program (Mark III Version). Vols. I and II. Rep. DAC 61552, (Air Force Contract Nos. F33615 67 C 1008 and F33615 67 C 1602), Douglas Aircraft Co., 1968. (Available from DDC as AD 851 811 and AD 851 812.)

6. Gray, J. Don, and Rhudy, R. W.: Investigation of Flat-Plate Aspect Ratio Effects on Ramp-Induced, Adiabatic, Boundary-Layer Separation at Supersonic and Hypersonic Speeds. AEDC-TR-70-235, 1971.

7. McDevitt, John B., and Rakich, John V.: The Aerodynamic Characteristics of Several Thick Delta Wings at Mach Numbers to 6 and Angles of Attack to 60°. NASA TM X-162, 1960.

8. Seiff, Alvin: Recent Information on Hypersonic Flow Fields. Proceedings of the NASA University Conference on the Science and Technology of Space Exploration, NASA SP-11, Vol. II, 1962, pp. 269-282.

9. Wawrzniak, M. E.: To What Extent Should Space Shuttle Stability and Control be Provided Through Stability Augmentation? Space Transportation System Technology Symposium, NASA TM X-52876, Vol. I, 1970, pp. 47-66.
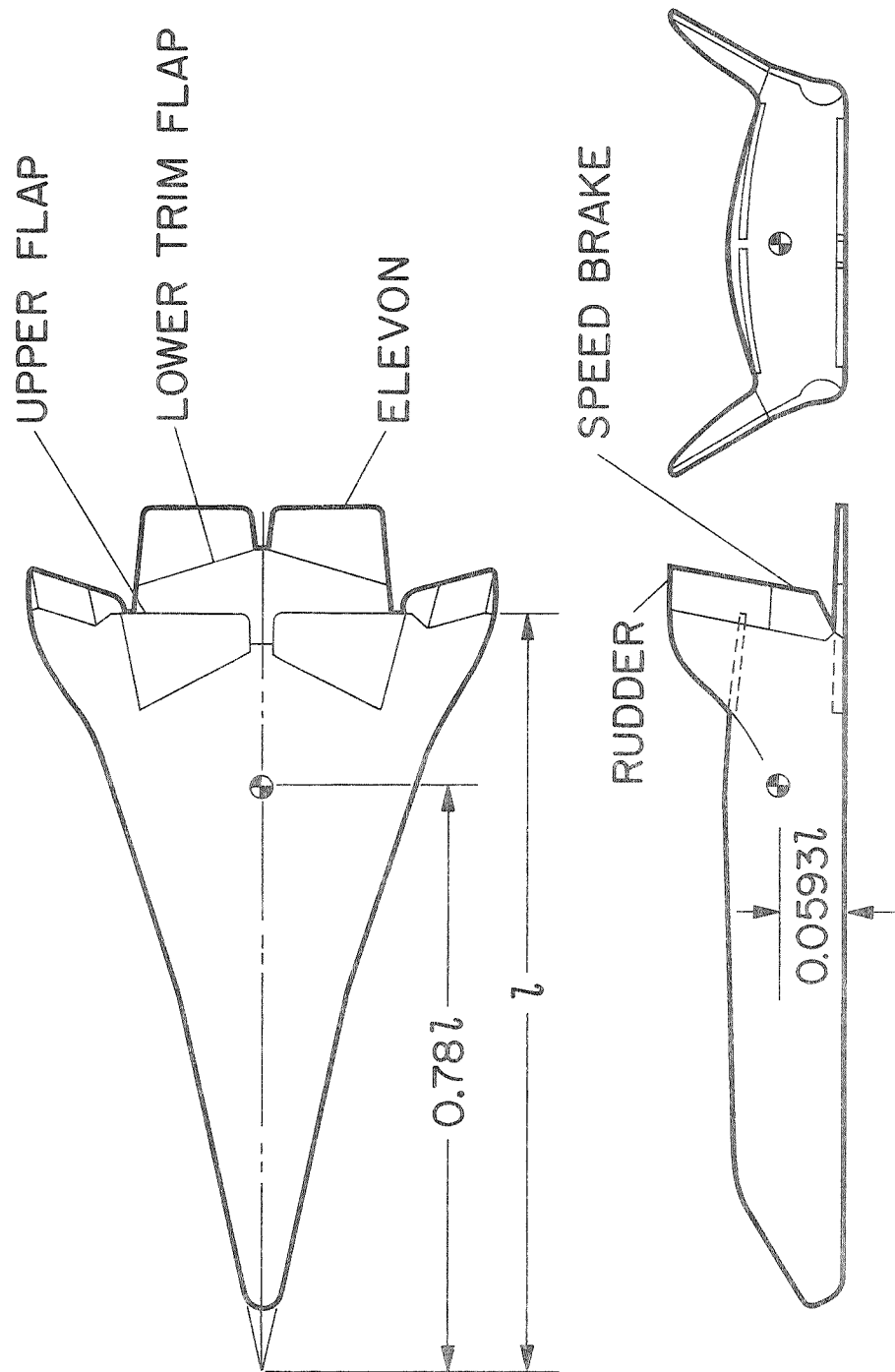
UPPER FLAP

LOWER TRIM FLAP

ELEVON

SPEED BRAKE

RUDDER

$0.781l$

l

$0.0593l$

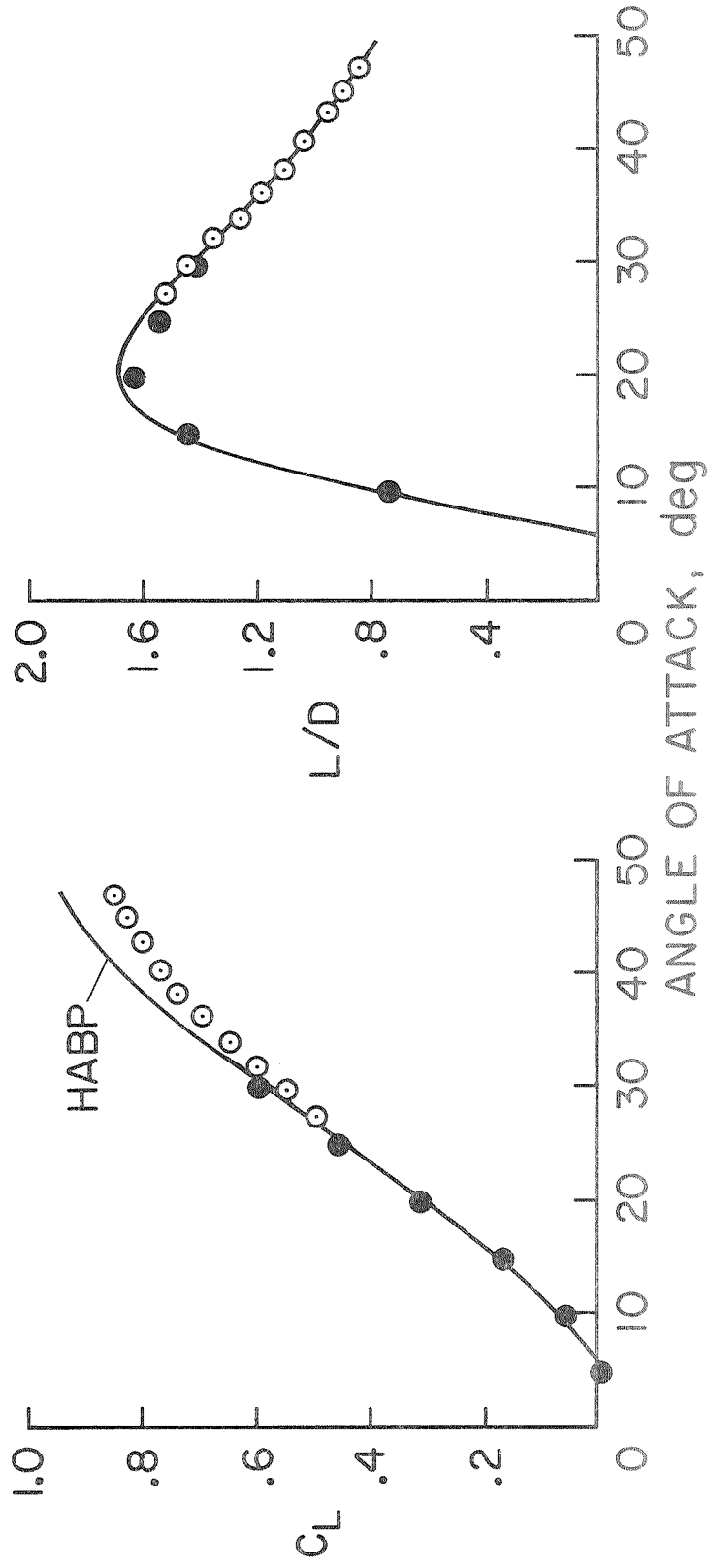Figure 1.— Sketch of the Lockheed LS-200-5 delta-body orbiter.

Figure 2.— Comparison of predicted and measured lift coefficient and lift-drag ratio.
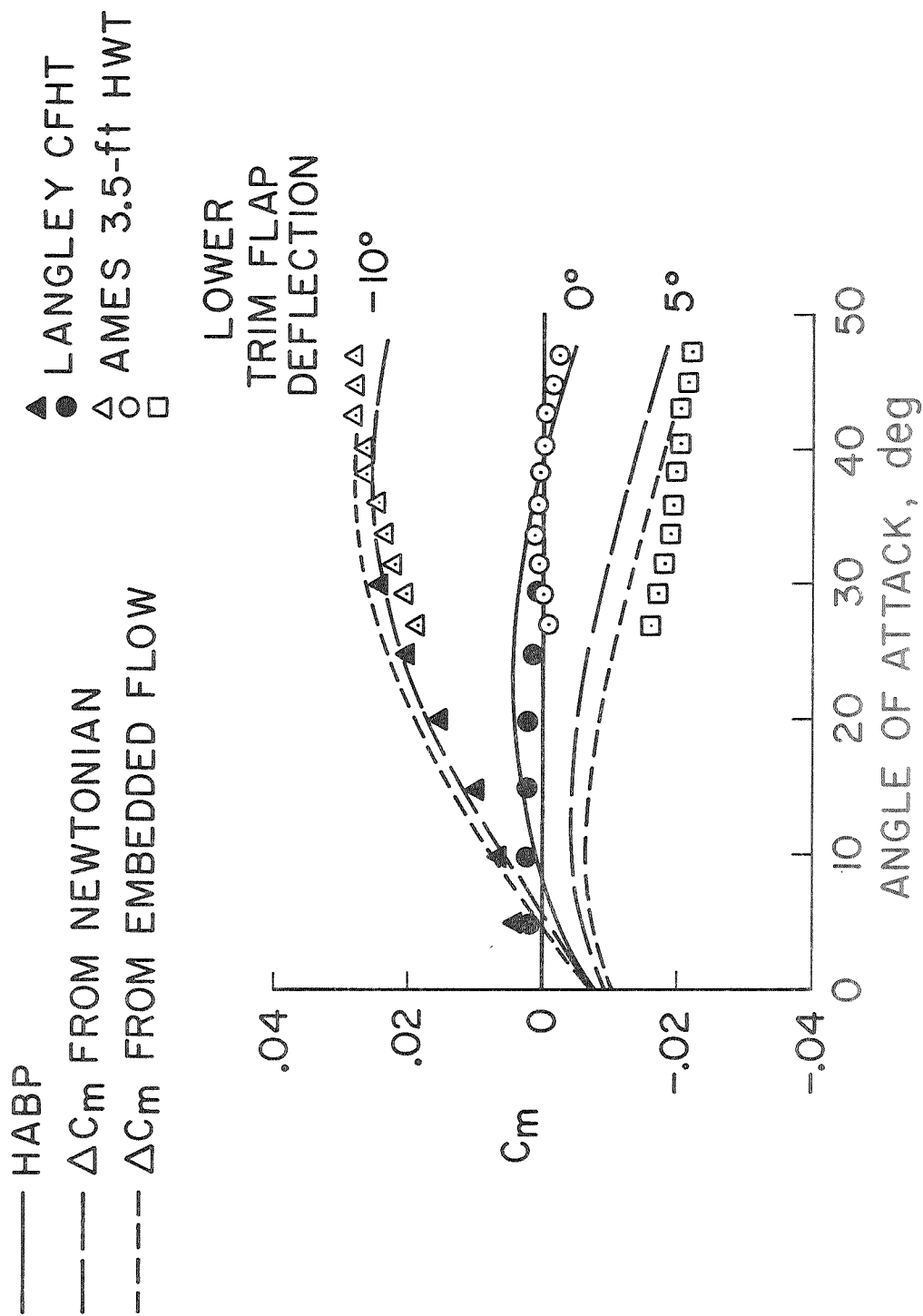
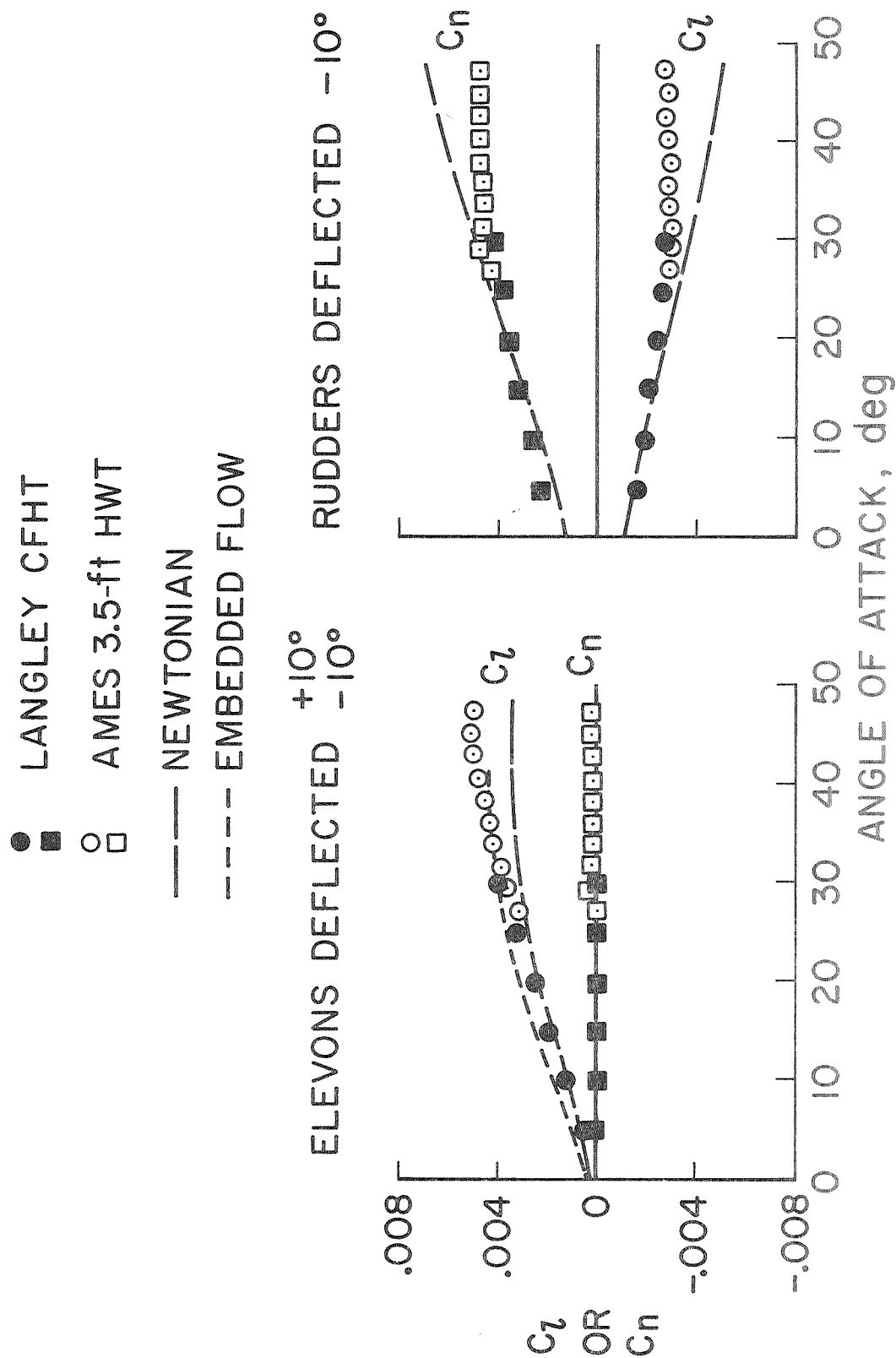Figure 3.— Comparison of predicted and measured longitudinal control characteristics.

Figure 4.— Comparisons of predicted and measured lateral-directional control characteristics.
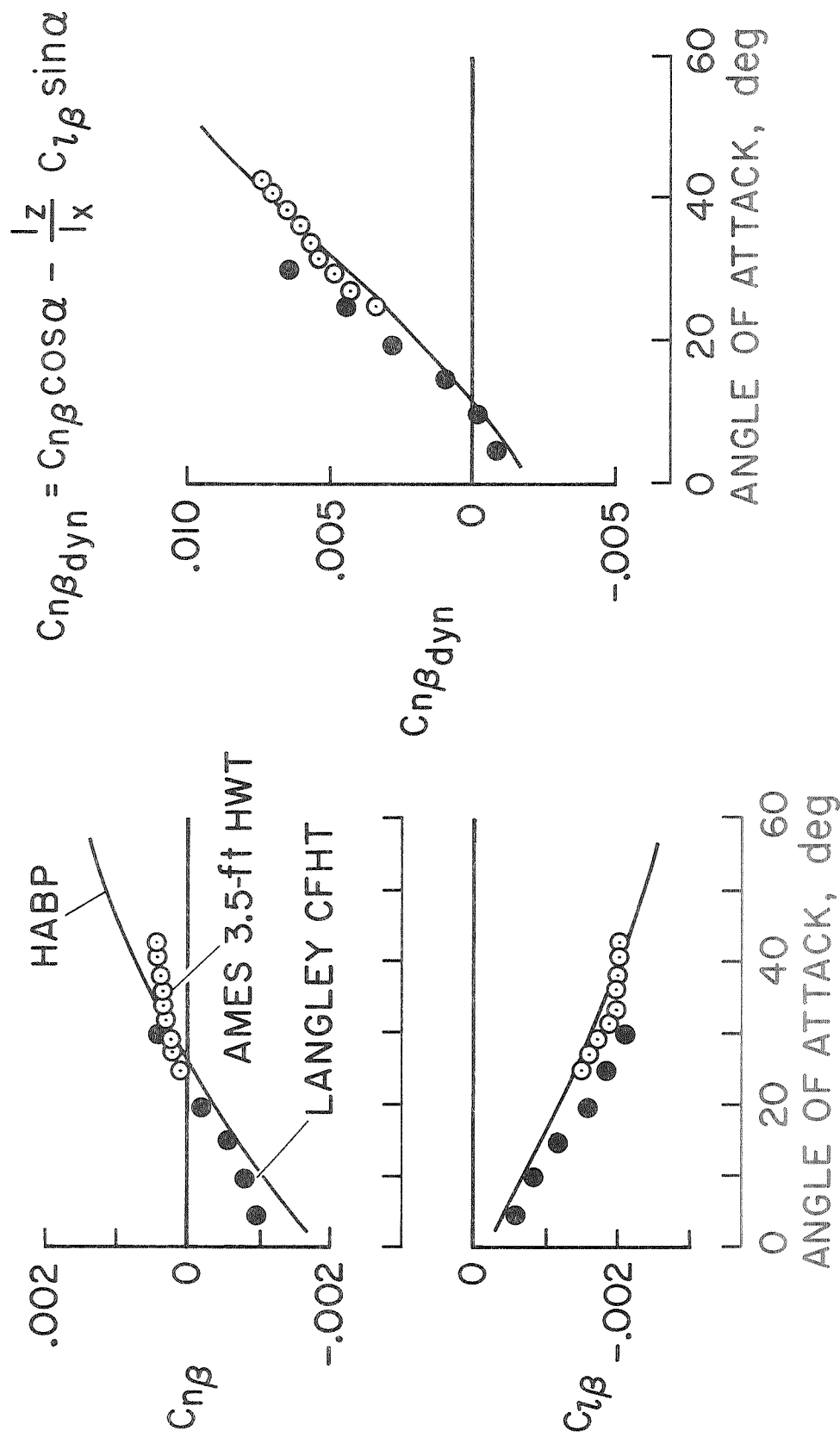
$$C_{n_{\beta_{dyn}}} = C_{n_\beta}\cos\alpha - \frac{I_z}{I_x} C_{l_\beta}\sin\alpha$$

Figure 5.– Comparison of predicted and measured lateral–directional stability.